Intrinsic fluorescence and energy transfer mechanisms in TbF3

M.F. Joubert, B. Jacquier, R. Moncorge, G. Boulon

Classification
Physics Abstracts
78.55

Intrinsic fluorescence and energy transfer mechanisms in TbF_3

M. F. Joubert, B. Jacquier, R. Moncorge and G. Boulon

ER N° 10 du CNRS, Université Lyon I, 69622 Villeurbanne, France

(*Reçu le 25 septembre 1981, accepté le 18 février 1982*)

Résumé. — Les mécanismes de transfert d'énergie dans TbF_3 sont examinés. L'excitation sélective laser est utilisée pour l'enregistrement des spectres continus et résolus dans le temps ainsi que pour l'étude des déclins de la fluorescence bleue $^5D_4 \rightarrow {}^7F_6$, à basse température. A 4,4 K, la fluorescence issue des niveaux pièges est la plus intense, alors qu'à 10 K la fluorescence intrinsèque domine. A partir des résultats expérimentaux, un modèle de diffusion mettant en jeu des pièges peu profonds est proposé pour élucider les processus de transfert d'énergie dans TbF_3. Finalement, la validité de ce modèle est discutée avec l'évaluation des paramètres. Un régime de diffusion rapide, sans transfert direct à grande distance, semble être le principal mécanisme à basse température.

Abstract. — The energy transfer mechanisms in TbF_3 have been investigated. The continuous and time resolved emission and excitation spectra as well as the decays of the blue fluorescence $^5D_4 \rightarrow {}^7F_6$ were measured at low temperature by using selective laser excitation. At 4.4 K most of the emission originates from traps while at 10 K the intrinsic fluorescence is stronger. On the basis of the experimental results a diffusion model involving shallow traps is proposed for the overall exciton to trap energy transfer process in TbF_3. Finally, the validity of the model is discussed with the evaluation of the parameters, and a fast diffusion regime without direct long range energy transfers seems to be the main mechanism at low temperature.

1. **Introduction.** — To obtain a high concentration of luminescent centres, generally required for applications such as mini lasers... one has to deal with so called « stoichiometric » materials. But, unfortunately, for any luminescent systems, a high activator concentration leads in general to a poor radiative efficiency. Assuming that this effect arises from the ion-ion interaction, it follows the relevant questions as the nature of the interaction and the physical mechanism which causes energy transfer among luminescent centres. Despite a significant amount of work that has been done recently, there are still some aspects of the fluorescence decay of concentrated terbium materials that are not well understood. To date, basic mechanisms have been proposed to explain the concentration quenching characteristics of stoichiometric materials [1]. Since we are dealing with terbium where the emitting levels are well separated from the fundamental multiplet, cross relaxation mechanism cannot be effective at low temperatures. Crystal-field overlap mixing effects between Tb^{3+} ions can be ruled out by the observation that the oscillator strengths of the Tb^{3+} transitions are independent of concentration. A third suggestion for concentration quenching involves the up-conversion recombination, but such an effect should have a typical non linear response at high excitation intensity. Thus, this process should be vanishingly small when operating at low pumping rates. Finally, energy migration through resonant energy transfer among Tb^{3+} ions, followed by a trapping mechanism to radiative traps and other quenching centres has been proposed.

In this paper we report the results of an investigation of the optical properties of TbF_3 where we have used some recent spectroscopic techniques in an attempt to better understand the energy transfer mechanisms in stoichiometric terbium materials in general. Time resolved fluorescence under selective excitation was used to identify the impurity induced fluorescence lines and to follow the temperature dependence of their intensities. Another technique involves the detailed analysis of the fluorescence decay following pulsed excitation. A model based on a rapid diffusion and trapping mechanism is consistent both with the spectral data and the observed decay modes.

2. **Sample and experimental equipment.** — The TbF_3 single crystal was grown in Hughes laboratory by a Czochralski technique. The sample was of good optical quality with typical dimensions of $3 \times 5 \times 5$ mm^3; a

thin plate of 1.14 mm thick was specially used for the absorption measurements. As it is well known impurities are always present even in the « purest » materials; an analysis of TbF_3 showed the following major impurities by weight : < 30 ppm of Pr^{3+}, Gd^{3+}. This leads to impurity concentration of about 10^{18} ions/cm^3 with respect to a total Tb^{3+} ion concentration of 2×10^{22} ions/cm^3. The symmetry of this crystal is orthorhombic with a space group D_{2h}^{16} (Pnma), rare earth sites being in C_s environments [2]. Magnetization measurements [3] and neutron diffraction studies [4] have shown that orthorhombic TbF_3 orders ferromagnetically below $T_c = 3.95$ K. Therefore, most of the experiments described in this paper were carried out above T_c.

A liquid helium optical cryostat with a heating gas system and a regulator device allowing to vary the temperature from 1.6 to 50 K was used. A conventional iodine lamp along with a modulator permitted us to record absorption spectra in the blue range of the transition $^7F_6 \rightarrow {}^5D_4$ of Tb^{3+}. Photons transmitted through the sample were analysed by a lm Hilger and Watts high resolution (8 Å/mm) scanning monochromator followed by a 6256 S EMI fast photomultiplier with a S.20 response. Synchronous detection compared the signal after the photomultiplier with the signal after the modulator.

A frequency tripled Quantel model 481 infrared YAG : Nd^{3+} laser (pulse length = 10 ns, repetition rate 10 Hz and energy per pulse : up to 120 mJ at 3 550 Å) followed by a three amplifier stage dye laser (pulse length : 10 ns and linewidth 0.1 cm^{-1}) was used to excite resonantly the lowest component of the $^5D_4$ level. With the help of the ORTEC photon counting and sampling systems, we were able to resolve the emission and excitation spectra with a minimum time delay after the laser pulse of less than 500 ns and a gate width of few μs. The decay time measurements were realized using a fast Intertechnique Model IN90 multichannel analyser. Intensity *versus* time data could be recorded and processed in 256 channels with a maximum resolution of 2 μs per channel.

3. **Emission spectra and fluorescence decays.** — At 25 K, the absorption spectrum shows six main lines, arising from the $^5D_4$ manifold components of figure 1. The oscillator strength f of the transitions at 20 604 cm^{-1} has been calculated using the well known formula :

$$f = \frac{18\, mc\varepsilon_0}{\pi e^2 \hbar} \frac{n}{(n^2+2)^2} \frac{\int \alpha_E \, d_E}{N_0} \qquad (1)$$

where

$$\frac{18\, mc\varepsilon_0}{\pi e^2 \hbar} = 8.21 \times 10^{17} \text{ cm}^{-3}/\text{eV mm}^{-1},$$

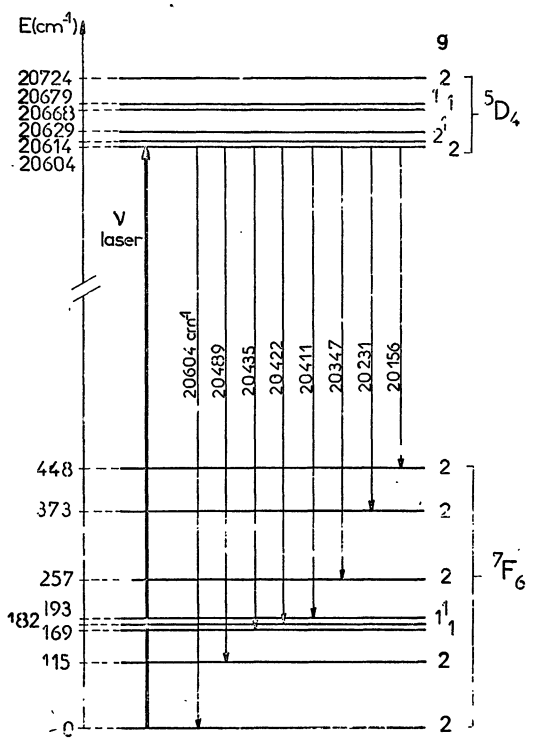

Fig. 1. — Stark components of the $^5D_4$ and $^7F_6$ energy levels of Tb^{3+} ion in TbF_3. They are deduced from absorption and emission spectra at 25 K. g = 1, 2 indicate singlet or quasidoublet component respectively.

n is the refractive index of the crystal, α_E the absorption coefficient at the energy E and N_0 the Tb^{3+} ion concentration. We find $f = 1.5 \times 10^{-9}$. This oscillator strength, characteristic of the 4 f^n magnetic dipole transitions, permits to compute a radiative lifetime of about 7 ms. This correlates quite well with the value of the limit lifetime at low temperatures (6 ms). From the blue emission spectra recorded with selective excitation in the lowest component of the $^5D_4$ level located at 20 604 cm^{-1} using a laser beam of less them 0.1 mJ pulse power, we can deduce the positions of the $^7F_6$ Stark components (Fig. 1) at 25 K. These results agree well with the values found by L. A. Bumagina *et al.* [5].

By decreasing the temperature from 25 K down to 5 K, the emission spectra show, below 15 K, new groups of lines located around 20 560, 20 470, 20 390 and 20 250 cm^{-1}. Moreover at 5 K, the intensity of these lines becomes stronger than any other (see Fig. 2*a*). By cooling the sample down to 1.6 K, new changes in the relative intensities of the fluorescence lines occur. These changes have been related to the magnetic ordering wich appears below 3.95 K [3]; but, this being out of the present subject, we shall concentrate ourselves only on the data obtained above this temperature. However, later on, we will use the observation of the extralines observed at 1.6 K, close to the resonant ones, as a proof of the existence of shallow traps. Such a temperature dependence of the emission

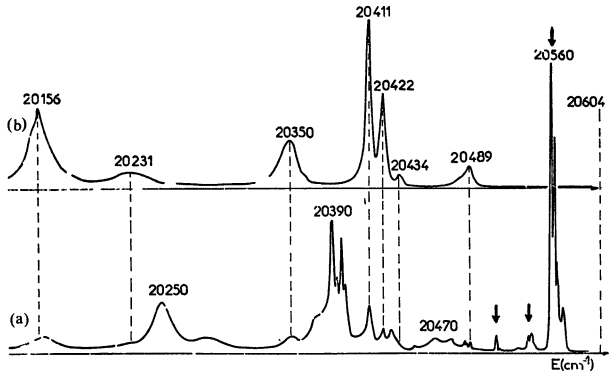

Fig. 2. — $^5D_4 \rightarrow {}^7F_6$ emission spectra at 5 K under excitation in the lowest Stark component of the $^5D_4$ level. *a*) Integrated spectrum $\left(\int I\,dt\right)$; *b*) Time resolved spectrum (delay of 1 μs, gate of 5 μs width). The arrows indicate the three series of impurity induced fluorescence lines, relative to the resonant line 20 604 cm^{-1}.

spectra is very similar to that observed by J. P. Van Derziel *et al.* [6] on a $Tb_3Al_5O_{12}$ crystal. To compare the time dependence of the intensities of the lines present at $T > 15$ K with those of the additional lines observed between 4.4 and 15 K, we use two different techniques : time resolved spectra and fluorescence decays. With a time delay after the laser pulse of 1 μs and a gate width of 5 μs, figure 2*b* shows clearly that the above mentioned additional lines are completely washed out of the spectrum.

Figures 3 and 4 exhibit the fluorescence decays, at 4.4 K, of the lines located at 20 600 and 20 560 cm^{-1} respectively after excitation in the lowest component of the $^5D_4$ level located around 20 604 cm^{-1}. Qualitatively, the decay of the first line is made of two parts : up

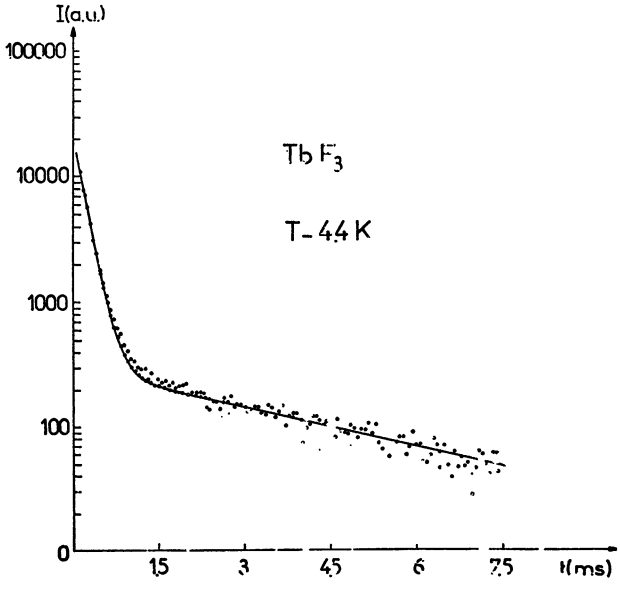

Fig. 3. — Decay curve of the intrinsic fluorescence line at 20 600 cm^{-1}. The points represent the experimental data and the curve is the fitting obtained using equation (7.1).

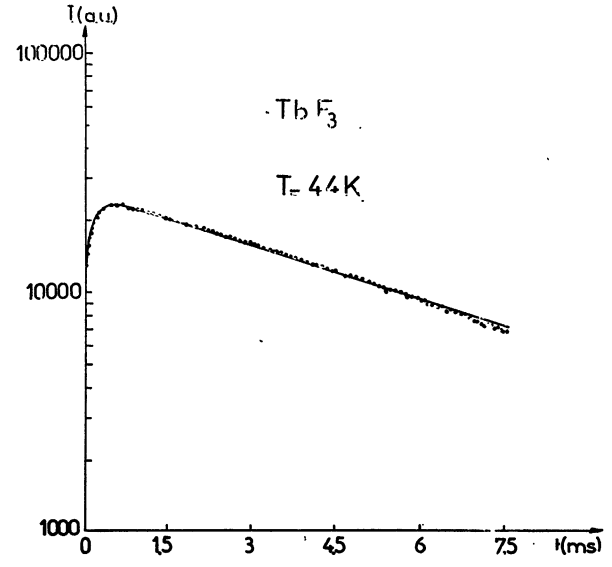

Fig. 4. — Time evolution of the trap fluorescence line at 20 560 cm^{-1}. The points represent the experimental data and the curve is the fitting obtained using equation (9).

to ~ 800 μs the intensity decreases rapidly by two orders of magnitude, then it decays exponentially with a characteristic time constant of about 4 ms. The intensity of the second line mentioned above shows first a rise time behaviour up to ~ 800 μs and then the intensity decreases exponentially with a time constant of about 5.3 ms. When increasing temperature up to 8 K, this initial rise becomes shorter and the separation between the two parts of the fluorescence decay of the line located at 20 600 cm^{-1} disappears. In fact, the rise time behaviour of the line at 20 560 cm^{-1} images the initial decay of the line at 20 600 cm^{-1}. In addition, the excitation spectra of these two emissions are similar and correlate tightly with the $^5D_4$ energy level positions of the absorption spectrum (Fig. 1). Thus, it is clear that the energy level giving rise to the fluorescence at 20 560 cm^{-1} is populated through out the energy level giving rise to the fluorescence at 20 600 cm^{-1}, this later being provided directly by the laser pulse excitation.

4. **Interpretation.** — 4.1 SPECTRAL ASSIGNMENT. — The additional lines observed below 15 K have been attributed to the emission of perturbed Tb^{3+} ions, which have been populated through the unperturbed Tb^{3+} ions. This perturbation is probably due to the presence of the small quantity of rare earth impurities such as the praseodymium and gadolinium ions mentioned before. Differences in the size and in the electronic configuration of the rare earth impurity induce significant changes in the crystal field acting on the terbium ions. Thus, depending upon the proximity of the impurity to a particular terbium ion, it will create « perturbed » and « unperturbed » or so called intrinsic Tb^{3+} ions. Hence the positions and the splittings of the $^5D_4$ and ^7F_J levels, as well as the corresponding

intensities of the transitions, will not be necessarily the same. To estimate the perturbed Tb^{3+} ion concentration, we have calculated the separations between one given Tb^{3+} ion and its nearest neighbours. The results are presented in table I. The twelve nearest neighbours form a group well separated from the others ; thus, only those neighbours are assumed to be significantly perturbed by a substitutional impurity such as Pr^{3+} or Gd^{3+} ion. This remark leads to a perturbed Tb^{3+} ion concentration N of about 12 times the impurity concentration, i.e. 12×10^{18} ions/cm^3.

Table I. — *Nearest neighbours of a* Tb^{3+} *ion in* TbF_3.

2	first	neighbours at 3.665 9 Å
2	second	neighbours at 3.915 6 Å
2	third	neighbours at 4.230 6 Å
4	fourth	neighbours at 4.381 7 Å
2	fifth	neighbours at 4.384 0 Å
2	sixth	neighbours at 5.485 7 Å
2	seventh	neighbours at 5.931 6 Å
4	eighth	neighbours at 6.462 7 Å

By analysing figure 2, we observe three series of impurity induced fluorescence lines. Below the resonant line (20 604 cm^{-1}), the first one spreads over 10 cm^{-1} at around 20 560 cm^{-1}, the second and the third ones give rise to the emission lines located at about 20 540 cm^{-1} ($\Delta \simeq 60$ cm^{-1}) and 20 512 cm^{-1} ($\Delta \simeq 100$ cm^{-1}) respectively. The same series of lines are also observed for each intrinsic transition, but their assignement becomes difficult because of the great number of $^7F_6$ Stark components. The energy separation from intrinsic (unperturbed Tb^{3+} ions) and trap (perturbed Tb^{3+} ions) levels can be evaluated in several ways.

For instance, intrinsic and trap fluorescence lines located at 20 411 (a) and 20 390 cm^{-1} (b) respectively are spectrally separated by $\Delta = 21$ cm^{-1}. Thermalization between these two levels (a) and (b) gives rise to the following relation between their respective intensity :

$$\frac{I_a}{I_b} = \frac{A_a}{A_b} \frac{h\nu_a}{h\nu_b} \frac{N_a}{N_b} \qquad (2)$$

where A_a and A_b are their respective spontaneous radiative emission probability, $h\nu_a$ and $h\nu_b$ their energy separation from the ground state and N_a and N_b their respective population. From our experiments, $A_a \simeq A_b = \tau_0^{-1}$ where τ_0 is the limit lifetime at low temperature. With $N_a = N_b\, e^{-\Delta/kT}$, where $\Delta = h\nu_a - h\nu_b$, we obtain :

$$\frac{I_a}{I_b} = e^{-\Delta/kT}. \qquad (3)$$

Moreover, the total probability of deexcitation for level b is

$$\tau^{-1} = \tau_0^{-1} + W_{ba} \qquad (4)$$

with

$$W_{ba} = K\, e^{-\Delta/kT}. \qquad (5)$$

Consequently, as shown on figure 5, the energy gap Δ is deduced from the temperature dependences both of the relative intensity and the inverse lifetime τ^{-1} of the trap emission. We find values of 21.7 cm^{-1} and 21.6 cm^{-1} respectively, in good agreement with the measured energy gap of 21 cm^{-1}.

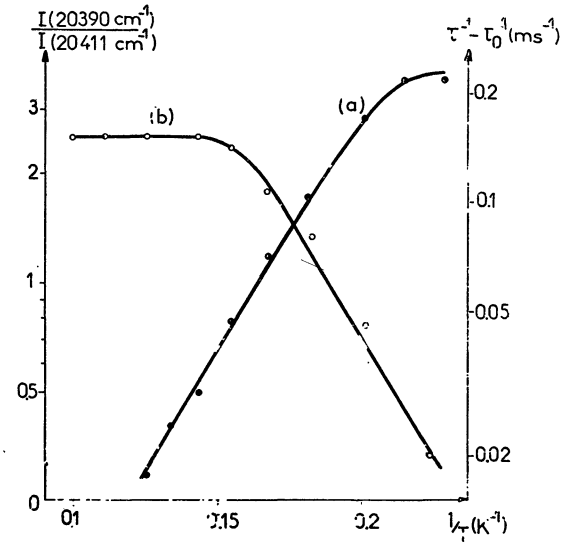

Fig. 5. — Temperature dependence of (*a*) the relative intensity of the trap line emission at 20 390 cm^{-1} with respect to the intensity of the intrinsic line emission at 20 411 cm^{-1} and (*b*) the inverse lifetime of perturbed Tb^{3+} emission at 20 390 cm^{-1}.

4.2 Model for the fluorescence. — The donor or intrinsic fluorescence decay presented above suggests a model in which the thermal depopulation of shallow traps is taken into account explicitly. It is found that this approach gives quantitatively a good image of the observations. Essentially, the same model has been worked out to describe qualitatively the impurity induced fluorescence of antiferromagnetic insulators [7, 8] and a similar model is well known for the exciton dynamics in the molecular crystals [9].

If we subtract the exponential function which describes the long time behaviour of the intrinsic decay (see Fig. 3), we find that, at short times, the intensity decreases exponentially with a characteristic time constant of 179 μs. This value correlates very well with that obtained in $TbPO_4$ [10] for the same excited level.

This leads us to consider the existence of weakly perturbed Tb^{3+} ions giving rise to shallow trap levels. Thus we propose to adopt the model presented schematically in figure 6. The majority of the Tb^{3+} ions forms the exciton band (level 2). As a consequence, the excitation energy is no more localized and the trapped levels (levels 1 and 0) are fed by energy transfer from the intrinsic exciton band. These considerations are consistent with the observation of identical excitation

spectra for both intrinsic and trap fluorescence and the tight correlation of these spectra with the absorption bands of the crystal.

We wish to calculate the population of levels 2, 1 and 0 as a function of time t. The transfer of excitation between the various levels is described in terms of transition rates which are shown in figure 6. Level 2 corresponds to the unperturbed Tb^{3+} ions responsible of the $^5D_4 \rightarrow {}^7F_6$ fluorescence line at 20 600 cm^{-1}. This intrinsic emission line corresponds to the lowest energy transition of the quadruplet (Fig. 1) which connects the lowest Stark components of $^5D_4$ and $^7F_6$; it was choosen because the integrated spectrum does not exhibit some particular impurity induced fluorescence line in the same spectral range (see Fig. 2). Levels 1 and 0 correspond to radiative traps. The first one is located very close to the unperturbed Tb^{3+} ion level, whereas the second gives rise to the fluorescence at 20 560 cm^{-1}. From the fluorescence spectra, the energy separation between levels 2 and 0 is $\sim$ 40 cm^{-1}. W_r is the radiative transition probability, W_q is the transition rate from level 2 to other deeper radiative and non radiative traps than level 0. The inverse transitions from level 1 to level 2 and from level 0 to level 2 require thermal phonons. The rates for these upward transitions are proportional to $\exp(-\Delta_1/kT)$ and $\exp(-\Delta_0/kT)$ respectively. In order to make our discussion easier, we make the following plausible assumptions : 1) The radiative transition probability W_r is the same for the perturbed and unperturbed ions. 2) The transition probability W_{02} is negligible at low temperature, below 7 K, due to the large energy separation $\Delta_0 \simeq 40$ cm^{-1}. 3) A trap cannot lose its energy directly to another trap. 4) The excitation which is trapped at a quenching trap is irretrievably lost for the system. Our experiments at low temperatures allow us to estimate the magnitude of W_{20}, W_{21} and W_r. The upward transition W_{02} being neglected, it follows under stationary conditions that : $N_2/N_0 = W_r/W_{20}$. The intensity from levels 2, 1 and 0 is simply given by $N_2 W_r$, $N_1 W_r$ and $N_0 W_r$ respectively. Since the integrated emission spectrum at 4.4 K (see Fig. 7) exhibits an intensity ratio of about 28 in

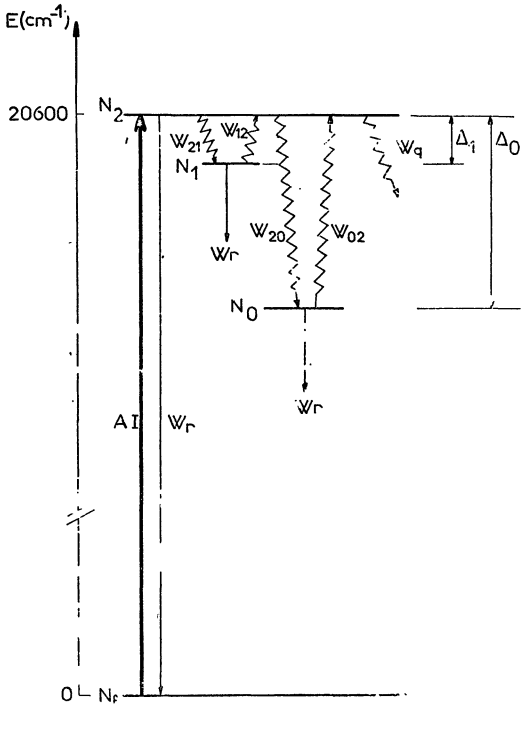

Fig. 6. — Schematic representation of the model.

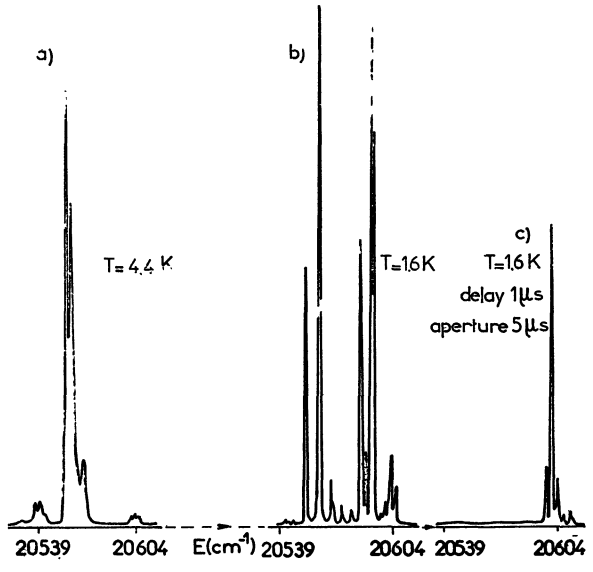

Fig. 7. — $^5D_4 \rightarrow {}^7F_6$ emission spectra near the resonant line at 20 604 cm^{-1}. *a*) Integrated spectrum $\left(\int I\,dt\right)$ at 4.4 K; *b*) Integrated spectrum $\left(\int I\,dt\right)$ at 1.6 K; *c*) Time resolved spectrum at 1.6 K (delay of 1 μs, gate width of 5 μs).

favour of the impurity induced fluorescence line, it means that W_r is small compared to W_{20}. Assuming that the tail of the intrinsic fluorescence decay is due to the influence of a particular shallow trap, the depth and the coupling strength of such a trap can be estimated by using the formulae (4) and (5). This leads to the values given in table II : thus, it is indicated that the coupling strength of this shallow trap is two order of magnitude smaller than for the deeper trap (of about 40 cm^{-1} deep), which justifies the additional condition : $W_{20} \gg W_{21}$.

Table II. — *Energy separation and coupling coefficient between the trap levels* (1 *and* 0) *and the intrinsic level.*

	Δ (cm^{-1})	K (s^{-1})
level 1	10	3.7×10^3
level 0	35	5.4×10^5

Taking into account these assumptions all together we are left with the following rate equations

$$\frac{dN_2}{dt} = W_{12} N_1 - (W_r + W_{21} + W_{20} + W_q) N_2 + N_f AI \tag{6.1}$$

$$\frac{dN_1}{dt} = W_{21} N_2 - (W_r + W_{12}) N_1 \tag{6.2}$$

$$\frac{dN_0}{dt} = W_{20} N_2 - W_r N_0 . \tag{6.3}$$

After the excitation pulse, and assuming that at $t = 0$, $N_1(0) = 0$ and $N_2(0)$ has a finite value; we get the following expressions :

$$N_2(t) = \frac{N_2(0)}{m_0}\left[\frac{W_{12}(W_{12} + W_{21} + 2W_r) + W_r^2}{m_0} e^{m_+ t} + (W_{21} + W_{20} + W_q) e^{m_- t}\right] \tag{7.1}$$

$$N_1(t) = \frac{N_2(0)}{m_0} W_{21}[e^{m_+ t} - e^{m_- t}] \tag{7.2}$$

where

$$m_0 = W_{21} + W_{12} + W_{20} + W_q + 2W_r \tag{8.1}$$

$$m_+ = -\left(W_r + \frac{W_{12}(W_{20} + W_q)}{m_0} - \frac{W_r^2}{m_0}\right) \tag{8.2}$$

$$m_- = -(W_{21} + W_{12} + W_{20} + W_q + W_r). \tag{8.3}$$

Using the following boundary condition for level 0 : $N_0(0) = 0$ at $t = 0$, the population $N_0(t)$ is given by :

$$N_0(t) = \frac{N_2(0)}{m_0} W_{20}\left[\frac{W_{12}(W_{12} + W_{21} + 2W_r) + W_r^2}{m_0(W_r + m_+)}(e^{m_+ t} - e^{-W_r t}) + \frac{W_{21} + W_{20} + W_q}{W_r + m_-}(e^{m_- t} - e^{-W_r t})\right]. \tag{9}$$

From equation (7.1) we have fitted the intrinsic fluorescence decay and obtained the values of the parameters $m_+ = -250\ s^{-1}$ and $m_- = -5\,586\ s^{-1}$ (Fig. 3). As a proof of the model, these values m_+ and m_- were used to describe the decay curve of the trap with the aid of equation (9). The fit to the data shown on figure 4 indicates a quite satisfactory agreement with the experiment. This agreement justifies the assumptions made previously and allows us to estimate the different non radiative rates from level 2 to the traps 1 and 0 and to the other sinks.

4.3 Evaluation of the parameters. — By using the temperature dependence of the exponential tail of the deeper trap fluorescence decay, from 4.4 to 7 K, we have previously deduced an energy gap $\Delta_0 \simeq 35\ cm^{-1}$. This compares favourably with the spectral energy separation of $40\ cm^{-1}$. From the thermal dependence of the exponential tail of the intrinsic fluorescence decay in the same temperature range, we have calculated an energy separation $\Delta_1 \simeq 10\ cm^{-1}$. This agrees nicely with the emission spectrum obtained at 1.6 K (Fig. 7) where a new group of lines appears located around $20\,591\ cm^{-1}$. From the experiment at 4.4 K, we know that $W_{20} \simeq 28\ W_r$, thus $W_{20} \simeq 4\,667\ s^{-1}$. Moreover, the experimental value of m_- is $-5\,586\ s^{-1}$. From equations (8.1) and (8.3) the expression of m_- allows calculation of $-(W_{21} + W_{12} + W_q)$ by the use of previous considerations on W_r and W_{20}. This leads to $W_{21} + W_{12} + W_q = 752\ s^{-1}$. This agrees with the above mentioned assumption $W_{21} \ll W_{20}$, and shows clearly the weak efficiency of energy transfer to non radiative sinks.

5. **Discussion.** — The model described in section 4 is consistent with all of the results obtained in this investigation. In the fast diffusion regime, the donor decay is essentially exponential with a rate constant

$$\tau^{-1} = \tau_0^{-1} + 4\pi D N_a \rho \tag{10}$$

where τ_0^{-1} is the radiative rate, D is the diffusion coefficient, N_a is the acceptor concentration and ρ is a length which characterizes the relative effectiveness of direct transfer and migration to traps. Following our assumptions, the initial portion of the intrinsic line decay (from few μs to 800 μs) decreases as $e^{m_- t}$

where m_- represents essentially the sum of all the transfer rates to radiative or quenching traps. Then, using formula (10) with a total trap concentration $N_a = 12 \times 10^{18}$ ions/cm^3 and $\rho = 4.16 \times 10^{-8}$ cm (calculated from the radius of the sphere of influence of an impurity), we find $D \simeq 8.6 \times 10^{-10}$ cm^2/s at 4.4 K. This value of D is one order of magnitude larger than in $Tb_3Al_5O_{12}$. In fact this situation seems to be reasonable, since the Tb environment in TbF_3 involves three times more Tb ions in the 5 Å sphere surrounding the cation than in $Tb_3Al_5O_{12}$. However, the approach used by Van der Ziel *et al.* [6] is fundamentally different from our proposed model since they deduced their diffusion coefficient D from the tail of the intrinsic fluorescence decay, using the Yokota and Tanimoto formalism [11] allowing for the competition of fast diffusion with direct long range energy transfer. The break observed in our decay curves (of the exciton) cannot be fitted following their expression for the time evolution of the intensity applicable over the complete time range :

$$N_2(t) = N_2(0) \exp\left[-\frac{t}{\tau_0} - \frac{4\pi^{3/2}}{3} N_a C^{1/2} t^{1/2} \times \left(\frac{1 + 10.87 z + 15.5 z^2}{1 + 8.743 z} \right)^{3/4} \right] \quad (11)$$

with $C = r_0^6/\tau_0$ where r_0 is the critical transfer radius, and $z = C^{-1/3} Dt^{2/3}$. This shows clearly the inadequacy of such a mechanism to reflete the decay curve of the donor fluorescence in the overall range of time (from few μs to several ms).

Furthermore, our model shows the different efficiencies of the traps; this can be discussed in terms of ion-ion interaction. It is known that exchange, electric multipole or magnetic dipole-dipole interactions mainly contribute to the diffusion mechanism [12]. However because of the selection rules, the EMI interaction cannot transfer excitations between $^7F_6$ and $^5D_4$ except *via* small admixtures of ^5G in the ground state and ^7F in the $^5D_4$ manifold. The exchange or magnetic dipole-dipole interactions would qualitatively explain the difference in the coupling strengths between deep traps involving the nearest neighbours and shallow traps involving the next nearest neighbours.

This aspect of the migration in TbF_3 will be shortly developed by analysing the time evolution of the exciton decay at very short times ($t < 1$ μs). As we have pointed out recently [13], the non linear behaviour of the blue fluorescence, under high pumping rate, is related to the existence of an up-conversion process. We believe that a further study of this effect would be also of great interest for a detailed determination of the Tb-Tb interactions involved.

Acknowledgments. — The authors are grateful to M. Blanchard, C. Madej and A. Lagriffoul for their technical assistance.

Thanks are also expressed to Mr Robinson (Hughes Laboratory) for having kindly provided us with the single crystal used here.

References

[1] For an up to date review of luminescent energy transfer and many references to theoretical and experimental work, see
AUZEL, F., *Radiationless processes*, edited by B. Di Bartolo (Plenum Press, New York) 1979, p. 213.

[2] ZALKIN, A. and TEMPLETON, D. H., *J. Am. Chem. Soc.* **75** (1953) 2453.

[3] HOLMES, L., GUGGENHEIM, H. J. and HULL, G. W., *Solid State Commun.* **8** (1970) 2005.

[4] PIOTROWSKI, M. and MURASIK, A., *Phys. Status Solidi* (a) **60** (1980) K 195.

[5] BUMAGINA, L. A., KAZAKOV, B. N., MALKIN, B. Z. and STOLOV, A. L., *Sov. Phys. Solid. State* **19** (1977) 624.

[6] VAN DER ZIEL, J. P., KOPF, L. and VAN UITERT, L. G., *Phys. Rev. B* **6** (1972) 615.

[7] DIETZ, R. E., JOHNSON, L. F. and GUGGENHEIM, H. J., *Physics of Quantum Electronics*, edited by Kelley P. L., Lax B. and Tannenwald P. E. (Mc Graw-Hill Book Co., New York) 1966, p. 361.

[8] GREENE, R. L., SELL, D. D., FEIGELSON, R. S., IMBUSCH, G. F. and GUGGENHEIM, H. J., *Phys. Rev.* **171** (1968) 600.

[9] DAVYDOV, A. S., *Sov. Phys. Usp.* **7** (1964) 145.

[10] DIGGLE, P. C., GEHRING, K. A. and MACFARLANE, R. M., *Solid State Commun.* **18** (1976) 391.

[11] YOKOTA, M. and TANIMOTO, O., *J. Phys. Soc. Japan* **22** (1967) 779.

[12] CONE, R. L. and MELTZER, R. S., *J. Chem. Phys.* **62** (1975) 3573.

[13] JOUBERT, M. F., JACQUIER, B., BOULON, G. and MONCORGE, R., 3th D.P.C. Conference Regensburg (1981), to be published in *Bull. Am. Phys. Soc.*